

## Nonlinear optimization for a tumor invasion PDE model

**A. A. I. Quiroga · G. A. Torres · D. Fernández · C. V. Turner**

Received: date / Accepted: date

**Abstract** In this work we introduce a methodology in order to approximate unknown parameters that appear on a non-linear reaction-diffusion model of tumor invasion. These equations consider that tumor-induced alteration of micro-environmental pH furnishes a mechanism for cancer invasion. A coupled system reaction-diffusion explaining this model is given by three partial differential equations for the non-dimensional spatial distribution and temporal evolution of the density of normal tissue, the neoplastic tissue growth and the excess concentration of  $H^+$  ions. The tumor model parameters have a corresponding biological meaning: the reabsorption rate, the destructive influence of  $H^+$  ions in the healthy tissue, the growth rate of tumor tissue and the diffusion coefficient.

We propose to solve the direct problem by using the Finite Element Method (FEM) and minimize an appropriate functional including both the real data (obtained via in-vitro experiments and fluorescence ratio imaging microscopy) and the numerical solution. The gradient of the functional is computed by the adjoint method.

---

The work of the authors was partially supported by grants from CONICET 2012-2015, SECYT-UNC 2015 and AGENCIA PICT-2014.

A. A. I. Quiroga

Centro Atómico Bariloche, CNEA, Bustillo km. 9.5 – CRUB-UNCo, Quintral 1250; San Carlos de Bariloche (8400) Rio Negro, Argentina.

E-mail: [aiquiroga@famaf.unc.edu.ar](mailto:aiquiroga@famaf.unc.edu.ar)

G. A. Torres

Facultad de Ciencias Exactas y Naturales y Agrimensura, Universidad Nacional del Nordeste, IMIT-CONICET, Av. Libertad 5470 (3400) Corrientes, Argentina.

E-mail: [torres@famaf.unc.edu.ar](mailto:torres@famaf.unc.edu.ar)

D. Fernández · C. V. Turner

Facultad de Matemática, Astronomía y Física, Universidad Nacional de Córdoba, CIEM-CONICET, Medina Allende s/n, Ciudad Universitaria (5000) Córdoba, Argentina.

E-mail: {[@famaf.unc.edu.ar](mailto:dfernandez,turner)}

**Keywords** Reaction-diffusion equation · Tumor invasion · PDE-constrained optimization · Adjoint method · Finite Element Method

**Mathematics Subject Classification (2000)** 35Q92 · 35R30 · 65M60

## 1 Introduction

Cancer is one of the greatest killers in the world although medical activity has been successful, despite great difficulties, at least for some pathologies. A great effort of human and economical resources is devoted, with successful outputs, to cancer modeling, [9, 1, 4, 5, 8, 26].

Some comments on the importance of mathematical modeling in cancer can be found in the literature. In the work [5] it is mentioned that “Cancer modelling has, over the years, grown immensely as one of the challenging topics involving applied mathematicians working with researchers active in the biological sciences. The motivation is not only scientific as in the industrial nations cancer has now moved from seventh to second place in the league table of fatal diseases, being surpassed only by cardiovascular diseases.”

In this work we use the mathematical analyses first proposed in [13] which supports the acid-mediated invasion hypothesis, hence it is acquiescent to mathematical representation as a reaction-diffusion system at the tissue scale, describing the spatial distribution and temporal development of tumor tissue, normal tissue, and excess  $H^+$  ion concentration.

The model predicts a pH gradient extending from the tumor-host interface. The effect of biological parameters critical to controlling this transition is supported by experimental and clinical observations [21].

In [13] a model tumor invasion was introduced in an attempt to find a common, underlying mechanism by which primary and metastatic cancers invade and destroy normal tissues. This work is not attempting to model the large-scale morphological features of tumors such as central necrosis or modeling the genetic changes which result in transformation or seeking to understand the causes of these changes. Rather, it concentrates on the microscopic scale population interactions occurring at the tumor-host interface, reasoning that these processes strongly influence the clinically significant manifestations of invasive cancer. Specifically, this work hypothesizes that the metabolism of the neoplastic tissue increased acid production and the diffusion of that acid into surrounding healthy tissue creates a microenvironment where tumor cells survive and proliferate whereas normal cells are unable to remain viable. The progressive loss of layers of normal cells at the tumor-host interface facilitates tumor invasion. Key elements of this tumor invasion mechanism are low interstitial pH of tumors due to primitive metabolism and reduced viability of normal tissue in a pH environment favorable to tumor tissue.

These model equations depend only on a small number of cellular and sub-cellular parameters. Analysis of the equations shows that the model predicts a crossover from a benign tumor to one that is aggressively invasive as a dimensionless combination of the parameters increases through a critical value.

The dynamics and structure of the tumor-host interface in invasive cancers are shown to be controlled by the same biological parameters which generate the transformation from benign to malignant growth. A hypocellular interstitial gap, as we can see in Figure 1 [13, Figure 4a], at the interface is predicted to occur in some cancers.

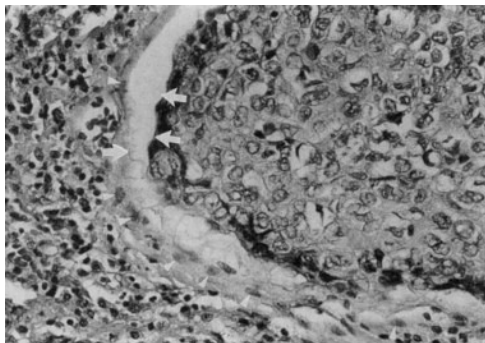


**Fig. 1** A micrographs of the tumor-host interface from human squamous cell carcinomas of the head and neck [13].

In [27], we develop an algorithm that allow us to estimate a unique parameter for a similar tumor model with a two dimensional spatial variable. Here we are interested in obtaining approximations for a pair of parameters that are related to the therapeutic, so we shall consider a one dimensional spatial variable in the tumor model.

In this paper we estimate a pair of parameters (the destructive influence of  $H^+$  ions in the healthy tissue and the control in the buffer process of  $H^+$  ions concentration) using an inverse problem. Moreover, via fluorescence ratio imaging microscopy, it is possible get data about the concentration of hydrogen ions [21]. We propose a framework via a PDE-constrained optimization problem, following the PDE-based model by Gatenby [13]. In this approach, tumor invasion is modeled via a coupled nonlinear system of partial differential equations, which makes the numerical solution procedure quite challenging.

This problem is a particular application of the inverse problems which are used in applied sciences: structured population dynamics [25], computerized tomography and image reconstruction in medical imaging [10,28], and more specifically tumor growth [2,16,19], among many others.

We solve a minimization problem using a gradient-based method considering the adjoint method in order to find the derivative of an objective functional. In this way, we would obtain the best parameters that fits patient-specific data.

The contents of this paper is organized into 8 sections as follows: Section 2 consists in some preliminaries about the model and the definition of the direct problem. Section 3 deals with the variational formulation of the direct problem. Section 4 considers the formulation of the minimization problem

and the reduced and adjoint problem, deriving the optimality conditions for the problem. Section 5 finds the gradient of the functional with respect to parameters that does not appear explicitly in the equation. Section 6 deals with the numerical solution of the adjoint problem, designing a suitable algorithm to solve it. In particular, we use the Finite Element Method. In Section 7 we show some numerical simulations to give information on the behavior of the functional and its dependence on the parameters including the corresponding tables. Section 8 presents the conclusions and some future work related to the contents of this paper.

## 2 Non-linear reaction-diffusion model of tumor invasion

We consider the mathematical model based on the theory of the change of the pH of the environment, proposed in [13]:

$$\frac{\partial N_1}{\partial t} = r_1 N_1 \left(1 - \frac{N_1}{K_1}\right) - d_1 L N_1, \quad (1)$$

$$\frac{\partial N_2}{\partial t} = r_2 N_2 \left(1 - \frac{N_2}{K_2}\right) + \nabla \cdot \left( D_{N_2} \left(1 - \frac{N_1}{K_1}\right) \nabla N_2 \right), \quad (2)$$

$$\frac{\partial L}{\partial t} = r_3 N_2 - d_3 L + D_{N_3} \Delta L, \quad (3)$$

which determine the spatial and temporal distribution of three variables:  $N_1(x, t)$ , the density of normal tissue;  $N_2(x, t)$ , the density of neoplastic tissue; and  $L(x, t)$ , the excess concentration of  $H^+$  ions. The units of  $N_1$  and  $N_2$  are cells/cm<sup>3</sup> and excess  $H^+$  ion concentration is expressed as a molarity (M),  $x$  and  $t$  are the position (in cm) and time (in seconds), respectively.

In equation (1) the behavior of the healthy tissue is determined by the logistic growth of  $N_1$  with growth rate  $r_1$  and carrying capacity  $K_1$ , and the interaction of  $N_1$  with excess  $H^+$  ions leading to a death rate proportional to  $L$ . The number  $d_1 L$  is the excess acid concentration, dependent death rate in accord with the well-described decline in the growth rate of normal cells, due to the reduction of pH from its optimal value of 7.4. The constants  $r_1$ ,  $d_1$  and  $K_1$  have units of 1/s, 1/(M s) and cells/cm<sup>3</sup>, respectively.

For equation (2), the neoplastic tissue growth is described by a reaction-diffusion equation. The reaction term is governed by a logistic growth of  $N_2$  with growth rate  $r_2$  and carrying capacity  $K_2$ . The diffusion term depends on the absence of healthy tissue with a diffusion constant  $D_{N_2}$ . Constants  $r_2$ ,  $K_2$  and  $D_{N_2}$  have units of 1/s, cells/cm<sup>3</sup> and cm<sup>2</sup>/s, respectively.

In equation (3), it is assumed that excess  $H^+$  ions are produced at a rate proportional to the neoplastic cell density, and diffuse chemically. An uptake term is included to take into account the mechanisms for increasing local pH (e.g., buffering and large-scale vascular evacuation [13]). Constant  $r_3$  is the production rate (M cm<sup>3</sup>/(cell s)),  $d_3$  is the reabsorption rate (1/s), and  $D_{N_3}$  is the  $H^+$  ion diffusion constant (cm<sup>2</sup>/s).

All the parameter values can be found in Table 1.

**Table 1** Parameter values used in [13].

Parameter	Estimate
$K_1$	$5 \times 10^7/\text{cm}^3$
$K_2$	$5 \times 10^7/\text{cm}^3$
$r_1$	$1 \times 10^{-6}/\text{s}$
$r_2$	$1 \times 10^{-6}/\text{s}$
$D_{N_2}$	$2 \times 10^{-10}\text{cm}^2/\text{s}$
$D_{N_3}$	$5 \times 10^{-6}\text{cm}^2/\text{s}$
$r_3$	$2.2 \times 10^{-17}\text{M cm}^3/\text{s}$
$d_3$	$1.1 \times 10^{-4}/\text{s}$

## 2.1 Nondimensionalization

Following the ideas exposed in [13], and considering one-dimensional space variables, the mathematical model is rescaled and the spatial and temporal domains are transformed onto the intervals  $I = (0, 1)$  and  $[0, T]$  respectively. Hence, let us define the following change of variables:

$$\begin{aligned} u_1 &= \frac{N_1}{K_1} & u_2 &= \frac{N_2}{K_2} & u_3 &= \frac{L}{L_0} \\ \tau &= r_1 t & \xi &= \sqrt{\frac{r_1}{D_{N_3}}} x \end{aligned} \quad (4)$$

where  $L_0 = r_3 K_2 / d_3$ . We will continue denoting  $x$  and  $t$  instead of  $\xi$  and  $\tau$ , respectively. Using the transformation (4) the dimensionless form of the equations (1)-(3) become

$$\frac{\partial u_1}{\partial t} = u_1(1 - u_1) - \delta_1 u_1 u_3, \quad (5)$$

$$\frac{\partial u_2}{\partial t} = \rho_2 u_2(1 - u_2) + \frac{\partial}{\partial x} \left( D_2(1 - u_1) \frac{\partial u_2}{\partial x} \right), \quad (6)$$

$$\frac{\partial u_3}{\partial t} = \delta_3(u_2 - u_3) + \frac{\partial^2 u_3}{\partial x^2}, \quad (7)$$

for  $(x, t) \in I \times (0, T]$ , where the four dimensionless quantities which parameterize the model are given by:

$$\delta_1 = \frac{d_1 r_3 K_2}{d_3 r_1}, \quad \rho_2 = \frac{r_2}{r_1}, \quad D_2 = \frac{D_{N_2}}{D_{N_3}}, \quad \delta_3 = \frac{d_3}{r_1}.$$

The interaction parameters between different cells (healthy and tumor) and concentration of  $\text{H}^+$  are difficult to measure experimentally. This is the reason for which we propose to estimate  $\delta_1$ . Also we will focus on  $\delta_3$  because we are interested in the buffering process that will allow to initiate the study of the therapeutic of this problem. The other parameters can be estimated by different techniques (see Table 1).

## 2.2 Initial and boundary conditions

At  $t = 0$  we will consider the tumor at a certain stage of its evolution. Hence the initial conditions are:

$$u_i(x, 0) = u_i^0(x), \quad i = 1, 2, 3, \quad (8)$$

for all  $x \in [0, 1]$ . We assume that the tumor is on the left of the domain, in the sense that the tumor cells are not moving. Then, for all  $t \in (0, T]$ , we have

$$\frac{\partial u_1}{\partial x}(0, t) = 0, \quad u_1(1, t) = 1, \quad (9)$$

$$\frac{\partial u_2}{\partial x}(0, t) = 0, \quad u_2(1, t) = 0, \quad (10)$$

$$\frac{\partial u_3}{\partial x}(0, t) = 0, \quad u_3(1, t) = 0. \quad (11)$$

From now on, equations (5)-(11) will be referred to as the direct problem.

## 2.3 Weak formulation of the direct problem

In this subsection we use  $\langle \cdot, \cdot \rangle$  to denote the duality pairing, i.e.,  $\langle \cdot, \cdot \rangle : U^* \times U \mapsto \mathbb{R}$  such that  $\langle w, u \rangle = w(u)$  (the space is always clear from the context), we emphasize that  $U^*$  is the space of continuous linear functionals over  $U$ .

Using the variational techniques for obtaining the weak solution of the direct problem [20,17,12], we can write the weak formulation of (5)-(11) as  $E(u, \omega) = 0$ , where  $E : U \times \mathbb{R}^2 \mapsto U^* \times (L^2(I))^3$  such that

$$\begin{aligned} \langle E(u, \omega), \zeta \rangle &= \int_{I_T} \left( \frac{\partial u_1}{\partial t} \lambda_1 - (1 - \tilde{u}_1 - u_1 - \delta_1 u_3)(\tilde{u}_1 + u_1) \lambda_1 \right) \\ &\quad + \int_{I_T} \left( \frac{\partial u_2}{\partial t} \lambda_2 - \rho_2 u_2 (1 - u_2) \lambda_2 + D_2 (1 - \tilde{u}_1 - u_1) \frac{\partial u_2}{\partial x} \frac{\partial \lambda_2}{\partial x} \right) \\ &\quad + \int_{I_T} \left( \frac{\partial u_3}{\partial t} \lambda_3 + \delta_3 (u_3 - u_2) \lambda_3 + \frac{\partial u_3}{\partial x} \frac{\partial \lambda_3}{\partial x} \right) \\ &\quad + \int_0^1 (\tilde{u}_1(0) + u_1(0) - u_1^0) \gamma_1 + \int_0^1 (u_2(0) - u_2^0) \gamma_2 \\ &\quad + \int_0^1 (u_3(0) - u_3^0) \gamma_3 \\ &= \left\langle \frac{\partial u}{\partial t} + F(u), \lambda \right\rangle + \langle u(0) - u^0, \gamma \rangle, \end{aligned} \quad (12)$$

where  $I_T = I \times [0, T]$ ,  $u = (u_1, u_2, u_3) \in U$ ,  $\tilde{u}(x, t) = \tilde{v}(x)$  with  $\tilde{v} \in (H^1(I))^3$  and  $\tilde{v}(1) = (1, 0, 0)$  is the Dirichlet lift,  $\omega = (\delta_1, \delta_3) \in \mathbb{R}^2$ ,  $\zeta = (\lambda, \gamma)$  with

$\lambda = (\lambda_1, \lambda_2, \lambda_3) \in U$ ,  $\gamma = (\gamma_1, \gamma_2, \gamma_3) \in (L^2(I))^3$ ,

$$U = \left\{ u \in L^2(0, T; V) \mid \frac{\partial u}{\partial t} \in L^2(0, T; V^*) \right\},$$

$$L^2(0, T; V) = \left\{ u : (0, T) \mapsto V \mid \int_0^T \|u(t)\|_{(H^1(I))^3}^2 < +\infty \right\},$$

with  $V = \{v \in (H^1(I))^3 \mid v(1) = 0 \in \mathbb{R}^3\}$  and  $H^1(I)$ ,  $L^2(I)$  are the standard Sobolev and Lebesgue function spaces, respectively. In summary, for  $u$  such that  $E(u, \omega) = 0$  we obtain that  $\tilde{u} + u$  is a weak solution of the direct problem.

### 3 The minimization problem

Suppose that in a time interval  $0 \leq t \leq T$  experimental information is available and that given a choice of  $\omega$  we represent by  $u$  the solution of the direct problem. Then, we propose to estimate  $\delta_1$  and  $\delta_3$  by solving the following inverse problem:

*Given available information over the time window  $0 \leq t \leq T$ , find a parameter  $\omega$  able to generate data  $u$  that best match the given data.*

First of all, we have to check which variables are observable, that is, which variables can be experimentally measured. In [21, 14] the authors proposed to measure the excess concentration of  $H^+$  ions at certain times  $t_k$ ,  $k = 1, \dots, M$  using fluorescence ratio imaging microscopy. We assume that we have observations of the dimensionless variable  $u_3$  that corresponds to the variable  $L$  (the excess concentration of  $H^+$  ions).

We define a distance (depending on the parameter  $\omega$ ) between the experimental data and the solution of the PDE system generated using  $\omega$  as a parameter. This distance is in fact an objective functional to be minimized. So, the functional  $J : U \times \mathbb{R}^2 \mapsto \mathbb{R}$  could be defined as:

$$J(u, \omega) = \frac{1}{2} \int_0^T \int_0^1 [u_3(x, t) - \hat{u}_3(x, t)]^2 \chi(t) dx dt, \quad (13)$$

where

$$\chi(t) = \sum_{k=1}^M e^{(-C(t-t_k)^2)},$$

is a weight function with  $C$  large enough,  $\hat{u}_3(x, t)$  is the excess concentration measured experimentally and  $u_3(x, t)$  is the excess concentration of  $H^+$  ions obtained by solving the direct problem for a certain choice of  $\omega$ .

Thus, we are interested in finding a solution of the PDE-constrained minimization problem

$$\begin{aligned} & \underset{(u, \omega) \in U \times \mathbb{R}^2}{\text{minimize}} && J(u, \omega) \\ & \text{subject to} && E(u, \omega) = 0, \\ & && \omega \in \Omega_{\text{ad}}, \end{aligned} \quad (14)$$

where  $\Omega_{\text{ad}}$  is the set of admissible values for  $\omega$ . In our case we can choose  $\Omega_{\text{ad}} = (0, \infty) \times (0, \infty)$ . Notice that the constraint  $E(u, \omega) = 0$  constitutes the direct problem.

There is a fundamental difference between the direct and inverse problem. Usually, inverse problems are ill-posed in the sense of existence, uniqueness and stability of the solution. Thus, regularization techniques can be considered [10, 11, 18].

### 3.1 The adjoint method

In the following, for a function  $F : U \times D \mapsto Z$  such that  $(u, \delta) \mapsto F(u, \delta)$ , we denote by  $F'(u, \delta)$  the full Fréchet-derivative and by  $\frac{\partial F}{\partial u}(u, \delta)$  and  $\frac{\partial F}{\partial \delta}(u, \delta)$  the partial Fréchet-derivatives of  $F$  at  $(u, \delta)$ . For a linear operator  $T : V \mapsto Z$  we denote by  $T^* : Z^* \mapsto V^*$  the adjoint operator of  $T$ .

We will consider the so-called reduced problem:

$$\begin{aligned} & \underset{\omega \in \mathbb{R}^2}{\text{minimize}} \quad \tilde{J}(\omega) = J(S(\omega), \omega) \\ & \text{subject to } \omega \in \Omega_{\text{ad}}, \end{aligned} \quad (15)$$

where  $\tilde{J} : \mathbb{R}^2 \mapsto \mathbb{R}$  and  $S : \Omega_{\text{ad}} \mapsto U$  is given as the solution of  $E(S(\omega), \omega) = 0$ . The existence of the function  $S$  is obtained by the implicit function theorem. According to the ideas exposed in [7, 15], this can be done since  $E$  is a continuously Fréchet-differentiable function, and assuming that for each  $\omega \in \Omega_{\text{ad}}$  there exists a unique corresponding solution  $u = S(\omega)$  such that the derivative  $\frac{\partial E}{\partial u}(S(\omega), \omega)$  is a continuous linear operator continuously invertible. Also, the solution of the problem (15) can be obtained by assuming that  $\Omega_{\text{ad}}$  is a compact set and  $J$  is a continuous function.

In order to find a minimum of the continuously differentiable function  $\tilde{J}$ , it will be important to compute the derivative of this reduced objective function. Hence, we will show a procedure to obtain  $\tilde{J}'$  by using the adjoint approach.

Since  $E(S(\omega), \omega) = 0$ , we have that  $\tilde{J}(\omega) = J(S(\omega), \omega) + \langle E(S(\omega), \omega), \zeta \rangle$ . Thus

$$\begin{aligned} \tilde{J}'(\omega) &= (S'(\omega))^* \left( \frac{\partial J}{\partial u}(S(\omega), \omega) + \left( \frac{\partial E}{\partial u}(S(\omega), \omega) \right)^* \zeta \right) \\ &\quad + \frac{\partial J}{\partial \omega}(S(\omega), \omega) + \left( \frac{\partial E}{\partial \omega}(S(\omega), \omega) \right)^* \zeta. \end{aligned}$$

For a given  $\omega$ , let us consider  $\zeta_\omega \in U \times (L^2(I))^3$  as the solution of the so-called adjoint problem:

$$\frac{\partial J}{\partial u}(S(\omega), \omega) + \left( \frac{\partial E}{\partial u}(S(\omega), \omega) \right)^* \zeta_\omega = 0. \quad (16)$$



Note that each term in (16) is an element of the space  $U^*$ . Therefore, for  $u_\omega = S(\omega)$  we obtain that

$$\tilde{J}'(\omega) = \frac{\partial J}{\partial \omega}(u_\omega, \omega) + \left( \frac{\partial E}{\partial \omega}(u_\omega, \omega) \right)^* \zeta_\omega, \quad (17)$$

where  $u_\omega$  and  $\zeta_\omega$  are solutions of the direct and adjoint problem, respectively.

Notice that in order to obtain  $\tilde{J}'(\omega)$  we need first to compute  $u_\omega$  by solving the direct problem, followed by the calculation of  $\zeta_\omega$  by solving the adjoint problem. For computing the second term of (17) it is not necessary to obtain the adjoint of  $\frac{\partial E}{\partial \omega}(u, \omega)$  but just its action over  $\zeta$ .

#### 4 Getting the derivative of the functional

In order to obtain the adjoint operator of  $\frac{\partial E}{\partial u}(u, \omega) : U \mapsto U^* \times (L^2(I))^3$ , recall that

$$\left\langle \left( \frac{\partial E}{\partial u}(u, \omega) \right)^* \zeta, \eta \right\rangle = \left\langle \frac{\partial E}{\partial u}(u, \omega) \eta, \zeta \right\rangle,$$

for any  $\eta \in U$  and  $\zeta \in U \times (L^2(I))^3$ . Since

$$\left\langle \frac{\partial E}{\partial u}(u, \omega) \eta, \zeta \right\rangle = \lim_{\mu \rightarrow 0} \frac{\langle E(u + \mu \eta, \omega), \zeta \rangle - \langle E(u, \omega), \zeta \rangle}{\mu},$$

after some algebraics, it can be shown that

$$\begin{aligned} \left\langle \frac{\partial E}{\partial u}(u, \omega) \eta, \zeta \right\rangle &= \int_{I_T} \left( \frac{\partial \eta_1}{\partial t} - (1 - 2(\tilde{u}_1 + u_1) - \delta_1 u_3) \eta_1 + \delta_1 (\tilde{u}_1 + u_1) \eta_3 \right) \lambda_1 \\ &\quad + \int_{I_T} \left( \frac{\partial \eta_2}{\partial t} - \rho_2 (1 - 2u_2) \eta_2 \right) \lambda_2 \\ &\quad + \int_{I_T} D_2 \left( -\frac{\partial u_2}{\partial x} \eta_1 + (1 - \tilde{u}_1 - u_1) \frac{\partial \eta_2}{\partial x} \right) \frac{\partial \lambda_2}{\partial x} \\ &\quad + \int_{I_T} \left( \frac{\partial \eta_3}{\partial t} - \delta_3 (\eta_2 - \eta_3) \right) \lambda_3 + \int_{I_T} \frac{\partial \eta_3}{\partial x} \frac{\partial \lambda_3}{\partial x} \\ &\quad + \int_0^1 (\eta_1(0) \gamma_1 + \eta_2(0) \gamma_2 + \eta_3(0) \gamma_3). \end{aligned}$$

Using integration by parts for time, we obtain

$$\begin{aligned} \left\langle \left( \frac{\partial E}{\partial u}(u, \omega) \right)^* \zeta, \eta \right\rangle &= \int_{I_T} \left( -\frac{\partial \lambda_1}{\partial t} - (1 - 2(\tilde{u}_1 + u_1) - \delta_1 u_3) \lambda_1 - D_2 \frac{\partial u_2}{\partial x} \frac{\partial \lambda_2}{\partial x} \right) \eta_1 \\ &\quad + \int_{I_T} \left( -\frac{\partial \lambda_2}{\partial t} - \rho_2 (1 - 2u_2) \lambda_2 - \delta_3 \lambda_3 \right) \eta_2 \\ &\quad + \int_{I_T} D_2 (1 - \tilde{u}_1 - u_1) \frac{\partial \lambda_2}{\partial x} \frac{\partial \eta_2}{\partial x} \end{aligned}$$

$$\begin{aligned}
& + \int_{I_T} \left( -\frac{\partial \lambda_3}{\partial t} + \delta_1(\tilde{u}_1 + u_1)\lambda_1 + \delta_3\lambda_3 \right) \eta_3 + \int_{I_T} \frac{\partial \lambda_3}{\partial x} \frac{\partial \eta_3}{\partial x} \\
& + \int_0^1 (\lambda_1(T)\eta_1(T) + (\gamma_1 - \lambda_1(0))\eta_1(0)) \\
& + \int_0^1 (\lambda_2(T)\eta_2(T) + (\gamma_2 - \lambda_2(0))\eta_2(0)) \\
& + \int_0^1 (\lambda_3(T)\eta_3(T) + (\gamma_3 - \lambda_3(0))\eta_3(0)).
\end{aligned}$$

On the other hand,

$$\left\langle \frac{\partial J}{\partial u}(u, \omega), \eta \right\rangle = \int_0^T \int_0^1 (u_3(x, t) - \hat{u}_3(x, t))\eta_3(x, t)\chi(t) dx dt.$$

Since  $\frac{\partial J}{\partial u}(u, \omega) + \left(\frac{\partial E}{\partial u}(u, \omega)\right)^* \zeta = 0$  if and only if  $\left\langle \frac{\partial J}{\partial u}(u, \omega) + \left(\frac{\partial E}{\partial u}(u, \omega)\right)^* \zeta, \eta \right\rangle = 0$  for all  $\eta \in U$ , we conclude that  $\zeta = (\lambda, \gamma)$  satisfies  $\frac{\partial J}{\partial u}(u, \omega) + \left(\frac{\partial E}{\partial u}(u, \omega)\right)^* \zeta = 0$  if and only if  $\gamma = \lambda(0)$ ,  $\lambda(T) = 0$  with  $\lambda \in U$  satisfying

$$\begin{aligned}
0 & = \int_{I_T} \left( -\frac{\partial \lambda_1}{\partial t} - (1 - 2(\tilde{u}_1 + u_1) - \delta_1 u_3)\lambda_1 - D_2 \frac{\partial u_2}{\partial x} \frac{\partial \lambda_2}{\partial x} \right) \eta_1 \\
& + \int_{I_T} \left( -\frac{\partial \lambda_2}{\partial t} - \rho_2(1 - 2u_2)\lambda_2 - \delta_3\lambda_3 \right) \eta_2 \\
& + \int_{I_T} D_2(1 - \tilde{u}_1 - u_1) \frac{\partial \lambda_2}{\partial x} \frac{\partial \eta_2}{\partial x} \\
& + \int_{I_T} \left( -\frac{\partial \lambda_3}{\partial t} + \delta_1(\tilde{u}_1 + u_1)\lambda_1 + \delta_3\lambda_3 + (u_3 - \hat{u}_3)\chi \right) \eta_3 \\
& + \int_{I_T} \frac{\partial \lambda_3}{\partial x} \frac{\partial \eta_3}{\partial x} \\
& = \left\langle -\frac{\partial \lambda}{\partial t} + H(\lambda), \eta \right\rangle, \tag{18}
\end{aligned}$$

for all  $\eta \in U$ . Thus, the weak formulation (18) shall be solved in order to get  $\zeta_\omega$ . Notice that the adjoint equations are posed backwards in time, with a final condition at  $t = T$ , while the state equations are posed forward in time, with an initial condition at  $t = 0$ .

Now, to compute the adjoint operator of  $\frac{\partial E}{\partial \omega}(u, \omega) : \mathbb{R}^2 \mapsto U^* \times (L^2(I))^3$ , for any  $q = (q_1, q_3) \in \mathbb{R}^2$  and  $\zeta \in U \times (L^2(I))^3$  we have

$$\begin{aligned}
\left\langle \left(\frac{\partial E}{\partial \omega}(u, \omega)\right)^* \zeta, q \right\rangle & = \left\langle \frac{\partial E}{\partial \omega}(u, \omega)q, \zeta \right\rangle \\
& = \lim_{\mu \rightarrow 0} \frac{\langle E(u, \omega + \mu q), \zeta \rangle - \langle E(u, \omega), \zeta \rangle}{\mu} \\
& = \int_{I_T} (\tilde{u}_1 + u_1)u_3\lambda_1 q_1 + \int_{I_T} (u_3 - u_2)\lambda_3 q_3.
\end{aligned}$$

On the other hand, since  $\frac{\partial J}{\partial \omega}(u, \omega) = 0$ , we obtain the following expression for (17),

$$\tilde{J}'(\omega) = \left( \frac{\partial E}{\partial \omega}(u_\omega, \omega) \right)^* \zeta_\omega = \begin{bmatrix} \int_{I_T} (\tilde{u}_1 + u_1) u_3 \lambda_1 \\ \int_{I_T} (u_3 - u_2) \lambda_3 \end{bmatrix}. \quad (19)$$

## 5 Algorithms for the direct and inverse problem

The minimization of the objective functional  $\tilde{J}$  (whose solutions are the model parameters) is an iterative procedure that needs the derivative of the objective functional. Solving two PDE problems (the direct and adjoint problems) per iteration we can obtain  $\tilde{J}'$ , which is cheaper than solving the direct problem many times per iteration to get the derivative [15]. We have implemented the algorithms in MATLAB, using the Finite Element Method for solving the direct and adjoint problems, and the Sequential Quadratic Programming (SQP) method for solving the optimization problem using the built-in function `fmincon`. At time  $t = 20$  and in terms of  $x$  variable, Figure 2 shows excess concentration of  $H^+$  ions, density of health cells and density of tumor cells.

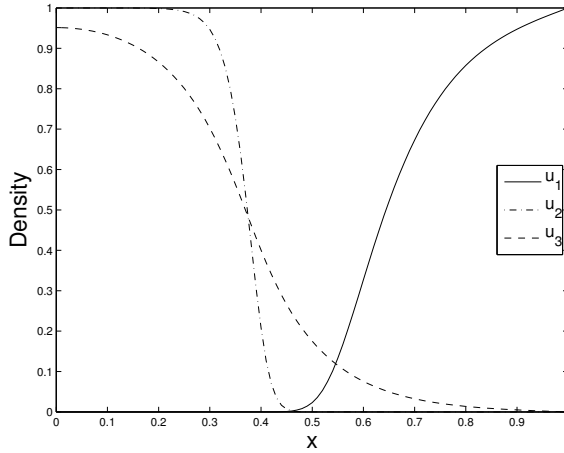


**Fig. 2** Density of health and tumor cells, and excess concentration of  $H^+$  ions at fixed time ( $t = 20$ ) with respect to  $x$  variable, for  $\delta_1 = 12.5$  and  $\delta_3 = 70$ .

In gradient-based optimization methods we need to have the derivative of the objective function [24]. The solution of the adjoint problem (once per iteration) allows to get the derivative regardless the number of inversion variables. Notice that the direct and adjoint problems can be solved by the Finite Element Method.

Below we present the procedure to minimize the functional  $\tilde{J}$ .

**Algorithm 51** *Adjoint-based minimization method.*

1. Give an initial guess  $\omega^0$  for the parameter.
2. In step  $k$ , given  $\omega^k$ , solve the direct and adjoint problems.
3. Get the derivative of the functional, i.e.  $\tilde{J}'(\omega^k)$ , using (19).
4. Obtain  $\omega^{k+1}$  by performing one iteration of the SQP method.
5. Stop using the criteria of `fmincon`.

To perform the minimization procedure, it is necessary to solve both the direct problem and the adjoint problem.

**Algorithm 52 Direct problem.**

1. Perform an implicit Euler step to find the state variables  $u$ , that is:

$$\frac{u(\cdot, t_n) - u(\cdot, t_{n-1})}{\tau} = F(u(\cdot, t_n)),$$

where  $t_n = t_{n-1} + \tau$ ,  $F(u(\cdot, t_n))$  is a nonlinear functional and the initial condition is  $u^0(x) = u(x, 0)$ .

2. Use FEM to make a discretization of  $u_i(x, t_n)$ :

$$u_i(x, t_n) \approx \sum_{j=1}^{nod} u_{i,j}^n \phi_j(x), \quad i = 1, 2, 3,$$

where  $\phi_j$  are the linear shape functions where and  $nod$  is the number of uniform distributed nodes for the spatial meshgrid for  $[0, 1]$ .

3. Calling  $U^n = [U_1^n, U_2^n, U_3^n] \in \mathbb{R}^q$ , where

$$U_i^n = [u_{i,1}^n, \dots, u_{i,j}^n, \dots, u_{i,nod}^n] \in \mathbb{R}^{nod}, \quad i = 1, 2, 3,$$

use the Newton method to find  $U^n \in \mathbb{R}^q$  such as  $U^n - U^{n-1} - \tau G(U^n) = 0$ , where  $G$  is the discretization of  $F$ .

**Algorithm 53 Adjoint problem.**

1. Perform an implicit Euler step to find the adjoint variable  $\lambda$ :

$$-\frac{\lambda(\cdot, t_n) - \lambda(\cdot, t_{n-1})}{\tau} = H(\lambda(\cdot, t_{n-1})),$$

where the final condition is  $\lambda(\cdot, T) = 0$ .

2. Use FEM to make a discretization of  $\lambda(\cdot, t_n)$  and solve the linear problem

$$\lambda^{n-1} - \lambda^n - \tau K(\lambda^{n-1}) = 0,$$

where  $K$  is the discretization of  $H$ .

## 6 Computational results

In this section we evaluate the performance of the adjoint-based optimization method proposed in this work. We show numerical simulations for some test cases using Algorithm 51.

Let us consider a synthetic experiment where  $\hat{u}_3(x, t)$  is generated via the direct model, for a choice of the model parameters  $\rho_2 = 1$ ,  $D_2 = 4 \times 10^{-5}$  and  $\hat{\omega} = (12.5, 70)$ . We choose  $\hat{\delta}_1 = 12.5$  with the objective of recovering the behavior of different cell densities as in Figure 1.

The graph of (15) in terms of  $\omega$  can be seen in Figure 3, leaving constant the other parameters. Notice that  $\tilde{J}$  looks convex with respect to  $\omega$ .

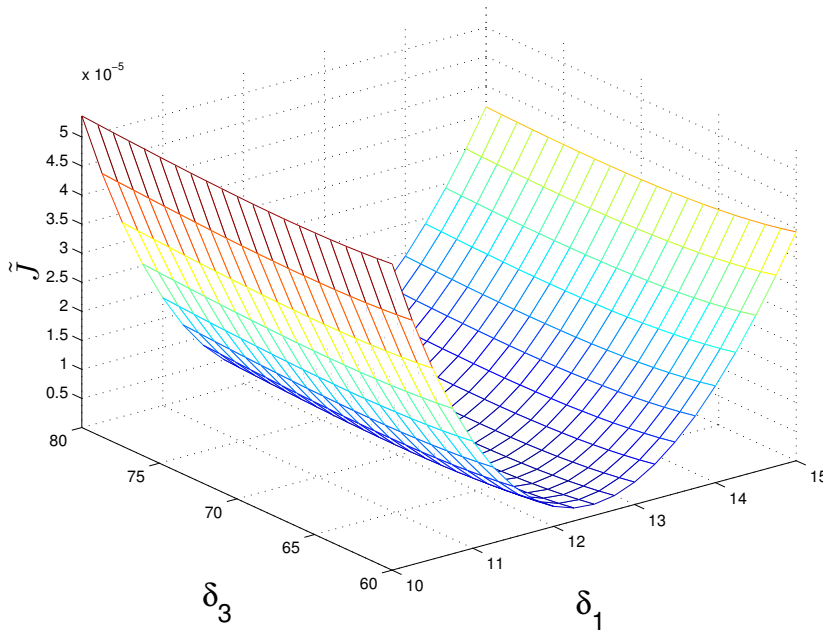


**Fig. 3** The functional  $\tilde{J}$  for  $\hat{u}_3$  generated with  $\hat{\omega} = (12.5, 70)$ .

We want to test if we can retrieve the original value of the parameter. This is not an easy task since we do not know, for instance, if the optimization problem has a solution, or if that solution is unique, or if the optimization problem has multiple local minima.

We have run Algorithm 51 for several values of  $\hat{\omega}$  where the initial condition  $\omega^0$  is randomly taken. Algorithms 52 and 53 were solved using the following algorithmic parameters:  $\tau = 0.5$ ,  $T = 20$ ,  $nod = 201$  and  $U_{ad} = [0, 20] \times [80, 120]$ . Results can be seen in Table 2) where we can observe that the retrieved parameter is obtained very accurately since the standard deviation is small.

**Table 2** Experiments for randomly initial data  $\omega^0$ ,  $\hat{\omega} = (12.5, 70)$ , where  $S$  is the standard deviation and  $e_{\delta_i}$  is the relative error

	$\bar{\omega}$	$S$	$e_{\delta_i}$
$\delta_1$	12.4749	1.5194	$6.6878^{-3}$
$\delta_3$	69.9732	$4.9359^{-2}$	$3.7610^{-4}$

**Table 3** Experiments for  $\hat{\omega} = (12.5, 70)$  and  $\sigma = 0.05$ , where  $S$  is the standard deviation and  $e_{\delta_i}$  is the relative error

	$\bar{\omega}$	$S$	$e_{\delta_i}$
$\delta_1$	13.2226	2.2095	$1.7215^{-2}$
$\delta_3$	70.1958	$8.5686^{-1}$	$2.7577^{-3}$

**Table 4** Experiments for  $\hat{\omega} = (12.5, 70)$  and  $\sigma = 0.08$ , where  $S$  is the standard deviation and  $e_{\delta_i}$  is the relative error

	$\bar{\omega}$	$S$	$e_{\delta_i}$
$\delta_1$	11.2916	2.8904	$9.9735^{-3}$
$\delta_3$	69.8592	$3.3723^{-1}$	$1.9819^{-3}$

**Table 5** Experiments for  $\hat{\omega} = (12.5, 70)$  and  $\sigma = 0.10$ , where  $S$  is the standard deviation and  $e_{\delta_i}$  is the relative error

	$\bar{\omega}$	$S$	$e_{\delta_i}$
$\delta_1$	11.7134	1.6167	$4.0346^{-3}$
$\delta_3$	69.9574	$7.8445^{-2}$	$5.9917^{-4}$

Since we have accurately retrieved the value of  $\hat{\omega}$  for different initial values  $\omega^0$ , we will consider  $\omega^0 = (8, 50)$  in the next experiment.

The presence of noise in the data (due for example to measurement errors) may imply strong numerical instabilities in the solution of an inverse problem [6]. One of the techniques to obtain values of  $\hat{u}_3$  is by fluorescence ratio imaging microscopy [21]. Measurement errors can be seen as random perturbations in the data.

Therefore, we can assume that we have observations of  $\hat{u}_3$  affected by Gaussian random noise with zero mean and standard deviation  $\sigma = 0.01, 0.05, 0.08, 0.1, 0.15$ . In Tables 3–6 we show, for each  $\sigma$ , the average  $\bar{\omega}$  over 10 values of  $\omega$ , the standard deviation  $S$  and the relative error for each parameters  $e_{\delta_i} = \frac{|\hat{\delta}_i - \bar{\delta}_i|}{\bar{\delta}_i}$ ,  $i = 1, 3$ .

## 7 Conclusions

A miscellany of new strategies, experimental techniques and theoretical approaches are emerging in the ongoing battle against cancer. Nevertheless, as

**Table 6** Experiments for  $\hat{\omega} = (12.5, 70)$  and  $\sigma = 0.15$ , where  $S$  is the standard deviation and  $e_{\delta_i}$  is the relative error

	$\bar{\omega}$	$S$	$e_{\delta_i}$
$\delta_1$	10.1207	3.2747	$2.6460^{-2}$
$\delta_3$	69.6646	$5.1785^{-1}$	$4.7218^{-3}$

new, ground-breaking discoveries relating to many and diverse areas of cancer modeling are made, scientists often have recourse to mathematical modeling in order to elucidate and interpret these experimental findings, [1, 5, 8, 3], and it became clear that these models are expected to success if the parameters involved in the modeling process are known. Or eventually, taking into account that some biological parameters may be unknown (especially in-vivo), the model can be used to obtain them [2, 10].

This paper, as already mentioned in Section 1, aims to offer a mathematical tool for the obtention of phenomenological parameters  $\delta_1$  and  $\delta_3$  representing the negative influence of the protons ions in the tissue (the acidification of the environment where live the cells) and the buffering (the way that the body naturally eliminate the exceeding of protons ions), respectively. These parameters can be identified by inverse estimation, by making suitable comparisons with experimental data. The inverse problem was stated as a PDE-constrained optimization problem, which was solved by using the adjoint method. In addition, the gradient of the proposed functional is obtained and can be extended, in principle, to any number of unknown parameters.

We remark that the parameter estimation via PDE-constrained optimization is a general approach that can be used, for instance, to consider the effects of nonlinear interaction between the health and tumor cells [23], and the buffering coefficient that allow us in a future to design a methodology to take into account the therapeutic of our problem.

As a future work we are interested in the dependence of the  $\delta_3$  on time, as in [22].

## References

1. Adam, J., Bellomo, N.: A survey of models for tumor immune systems dynamics. Modeling and simulation in science, engineering & technology. Birkhäuser (1997). URL <http://books.google.com/books?id=YBgmXkpWOp4C>
2. Agnelli, J.P., Barrea, A., Turner, C.: Tumor location and parameter estimation by thermography. *Mathematical and Computer Modelling* **53**(7), 1527–1534 (2011)
3. Araujo, R., McElwain, D.: A history of the study of solid tumour growth: the contribution of mathematical modelling. *Bulletin of Mathematical Biology* **66**(5), 1039–1091 (2004)
4. Bellomo, N., Chaplain, M.A.J., de Angelis, E.: Selected topics in cancer modeling: genesis, evolution, immune competition, and therapy. Springer Science & Business Media (2008)
5. Bellomo, N., Li, N., Maini, P.: On the foundations of cancer modelling: selected topics, speculations, and perspectives. *Mathematical Models and Methods in Applied Sciences* **18**(04), 593–646 (2008)

6. Bertero, M., Piana, M.: Inverse problems in biomedical imaging: modeling and methods of solution. In: *Complex systems in biomedicine*, pp. 1–33. Springer (2006)
7. Brandenburg, C., Lindemann, F., Ulbrich, M., Ulbrich, S.: A continuous adjoint approach to shape optimization for Navier Stokes flow. In: *Optimal control of coupled systems of partial differential equations*, pp. 35–56. Springer (2009)
8. Byrne, H.M.: Dissecting cancer through mathematics: from the cell to the animal model. *Nature Reviews Cancer* **10**(3), 221–230 (2010)
9. Cristini, V., Lowengrub, J.: *Multiscale modeling of cancer: an integrated experimental and mathematical modeling approach*. Cambridge University Press (2010)
10. van den Doel, K., Ascher, U.M., Pai, D.K.: Source localization in electromyography using the inverse potential problem. *Inverse Problems* **27**(2), 025,008 (2011)
11. Engl, H.W., Hanke, M., Neubauer, A.: *Regularization of inverse problems*, vol. 375. Kluwer Academic Pub (1996)
12. Evans, L.C.: *Partial differential equations* (1998)
13. Gatenby, R.A., Gawlinski, E.T.: A reaction-diffusion model of cancer invasion. *Cancer Research* **56**(24), 5745–5753 (1996)
14. Gatenby, R.A., Gawlinski, E.T., Gmitro, A.F., Kaylor, B., Gillies, R.J.: Acid-mediated tumor invasion: a multidisciplinary study. *Cancer Research* **66**(10), 5216–5223 (2006)
15. Hinze, M.: *Optimization with PDE constraints*, vol. 23. Springer (2009)
16. Hogeia, C., Davatzikos, C., Biros, G.: An image-driven parameter estimation problem for a reaction–diffusion glioma growth model with mass effects. *Journal of Mathematical Biology* **56**(6), 793–825 (2008)
17. Kinderlehrer, D., Stampacchia, G.: *An introduction to variational inequalities and their applications*. Society for Industrial and Applied Mathematics (1987)
18. Kirsch, A.: *An introduction to the mathematical theory of inverse problems*, vol. 120. Springer Science+ Business Media (2011)
19. Knopoff, D., Fernández, D., Torres, G., Turner, C.: Adjoint method for a tumor growth PDE-constrained optimization problem. *Computers & Mathematics with Applications* **66**(6), 1104–1119 (2013)
20. Ladyzhenskaiia, O.A., Solonnikov, V.A., Uraltseva, N.N.: *Linear and quasi-linear equations of parabolic type*, vol. 23. American Mathematical Soc. (1988)
21. Martin, G.R., Jain, R.K.: Noninvasive measurement of interstitial pH profiles in normal and neoplastic tissue using fluorescence ratio imaging microscopy. *Cancer Research* **54**(21), 5670–5674 (1994)
22. Martin, N.K., Gaffney, E.A., Gatenby, R.A., Maini, P.K.: Tumour–stromal interactions in acid-mediated invasion: a mathematical model. *Journal of Theoretical Biology* **267**(3), 461–470 (2010)
23. McGillen, J.B., Gaffney, E.A., Martin, N.K., Maini, P.K.: A general reaction–diffusion model of acidity in cancer invasion. *Journal of Mathematical Biology* pp. 1–26 (2013)
24. Nocedal, J., Wright, S.J.: *Numerical optimization*. Springer Science+ Business Media (2006)
25. Perthame, B., Zubelli, J.P.: On the inverse problem for a size-structured population model. *Inverse Problems* **23**(3), 1037–1052 (2007)
26. Preziosi, L.: *Cancer modelling and simulation*. CRC Press (2003)
27. Quiroga, A., Fernández, D., Torres, G., Turner, C.: Adjoint method for a tumor invasion PDE-constrained optimization problem in 2D using adaptive finite element method. *Applied Mathematics and Computation* **270**, 358 – 368 (2015)
28. Zubelli, J.P., Marabini, R., Sorzano, C., Herman, G.T.: Three-dimensional reconstruction by chahine’s method from electron microscopic projections corrupted by instrumental aberrations. *Inverse Problems* **19**(4), 933–949 (2003)